Lyle, M., Koizumi, I., Richter, C., and Moore, T.C., Jr. (Eds.), 2000
Proceedings of the Ocean Drilling Program, Scientific Results, Vol. 167

10. ALKENONE PALEOTHERMOMETRY AND ORBITAL-SCALE CHANGES IN SEA-SURFACE TEMPERATURE AT SITE 1020, NORTHERN CALIFORNIA MARGIN[1]

S.F. Kreitz,[2] T.D. Herbert,[2] and J.D. Schuffert[2]

ABSTRACT

$U_{37}^{k'}$ sea-surface temperature (SST) estimates obtained at ~2.5-k.y. resolution from Ocean Drilling Program Site 1020 show glacial–interglacial cyclicity with an amplitude of 7°–10°C over the last 780 k.y. This record shows a similar pattern of variability to another alkenone-based SST record obtained previously from the Santa Barbara Basin. Both records show that oxygen isotope Stage (OIS) 5.5 was warmer by ~3°C relative to the present and that glacial $U_{37}^{k'}$ temperatures warm in advance of deglaciation, as inferred from benthic $\delta^{18}O$ records. The alkenone-based SST record at Site 1020 is longer than previously published work along the California margin. We show that warmer than present interglacial stages have occurred frequently during the last 800 k.y. Alkenone concentrations, a proxy for coccolithophorid productivity, indicate that sedimentary marine organic carbon content has also varied significantly over this interval, with higher contents during interglacial periods. A baseline shift to warmer SST and greater alkenone content occurs before OIS 13.

We compare our results with those from previous multiproxy studies in this region and conclude that SST has increased by ~5°C since the last glacial period (21 ka). Our data show that maximum alkenone SSTs occur simultaneously with minimum ice volume at Site 1020, which is consistent with data from farther south along the margin. The presence of sea ice in the glacial northeast Pacific, the extent of which is inferred from locations of ice-rafted debris, provides further support for our notion of cold surface water within the northern California Current system, averaging 7°–8°C cooler during peak glacial conditions. The cooling of surface water during glacial stages most likely did not result from enhanced upwelling because alkenone concentrations and terrestrial redwood pollen assemblages are consistently lower during glacial periods.

INTRODUCTION

The California Current system (CCS) forms the eastern limb of the North Pacific Gyre. This complex system of opposing currents brings cool, fresh water to the tropics and exerts a strong influence on the climate of western North America (Lyle et al. 1992; Ramp et al., 1997; Norton and McLain, 1994; Dettinger et al., 1995). Physical processes such as Ekman transport, wind-stress curl, and ultimately thermohaline circulation (Hickey, 1979) enable the CCS to sense basinwide changes in ocean temperatures and wind fields. On historical time scales, this variability also affects coastal circulation, local fisheries, and rainfall along the western coast of North America (Hayward et al., 1996). On decadal time scales in the modern Pacific Ocean, periodic disturbances in basinwide wind fields, sea-surface temperatures (SST), and biological productivity are linked to El Niño/Southern Oscillation (ENSO) events that originate in equatorial regions (Chelton, 1982; Simpson, 1983; Emery and Hamilton, 1985). Typical ENSO conditions along the California margin include unusually warm SST and reduced coastal upwelling (Enfield, 1989), whereas cooler SST and strengthened coastal upwelling typify La Niña conditions. Whether these ENSO connections are analogs to glacial–interglacial cycles on longer, orbital time scales along the California margin remains an interesting but unanswered question. Improved paleoceanographic knowledge of the CCS on glacial–interglacial time scales will help to unlock the complexities between the interactions of wind fields, ice-sheet stability, and variations in the oceanic heat pump of the Pacific. Ocean Drilling Program (ODP) Site 1020 (Fig. 1), a pelagic drill site on the eastern flanks of the Gorda Ridge, lies directly under the CCS but far enough offshore to avoid influence by seasonal upwelling events (Lyle, Koizumi, Richter, et al., 1997). The excellent recovery of an undisturbed sedimentary section at this site provides an opportunity to characterize regional variations in oceanic circulation on orbital time scales.

The role of eastern boundary currents as fundamental components of basinwide oceanic circulation remains poorly understood on orbital time scales in the Pacific. One model suggests that eastern boundary currents may have strengthened during glacial times. CLIMAP Project Members (1981) reconstructed glacial SSTs throughout the oceans and saw markedly cooler water within the eastern boundary current along the coast of northwest Africa and in the Peru Chile Current. They concluded that the inferred cooling resulted from increased upwelling of subsurface water driven largely by more vigorous oceanic circulation.

The difficulty of obtaining paleoceanographic data along the California margin results largely from poor preservation of calcium carbonate ($CaCO_3$), an important component in almost all marine paleoreconstructions. CLIMAP Project Members (1981) used radiolarian faunal assemblages coupled with oxygen isotope ($\delta^{18}O$) stratigraphy to identify a Holocene to last glacial maximum (LGM) SST anomaly of 2°C in the North Pacific, but they characterized the entire region with only two cores. More recently, Sancetta et al. (1992) used diatom fauna, pollen, and sedimentological data from the Multitracers project and Lyle et al. (1992) to characterize the Holocene–LGM oceanographic variability of the northern CCS. They found that marine organic sediment contents (offshore) were lower during the LGM than at present, and their terrestrial pollen records north of 36°N suggested reduced upwelling during the LGM. Sabin and Pisias (1996) examined the marine-terrestrial link from a suite of cores in the latitudinal band of 35°–50°N and found that SST anomalies based on radiolarian transfer functions correlated well (warmer SST and warmer pollen-derived paleotemperatures) with terrestrial pollen records from the Pacific Northwest.

Our study uses sedimentary alkenones as indicators for overlying SST and marine productivity. As organic biomarkers, alkenones provide an excellent opportunity to characterize SSTs where traditional carbonate proxies are poorly preserved because their ratios resist sed-

[1]Lyle, M., Koizumi, I., Richter, C., and Moore, T.C., Jr. (Eds.), 2000. *Proc. ODP, Sci. Results,* 167: College Station TX (Ocean Drilling Program).
[2]Department of Geological Sciences, Box 1846, Brown University, Providence RI 02912, USA. Correspondence author: timothy_herbert@brown.edu

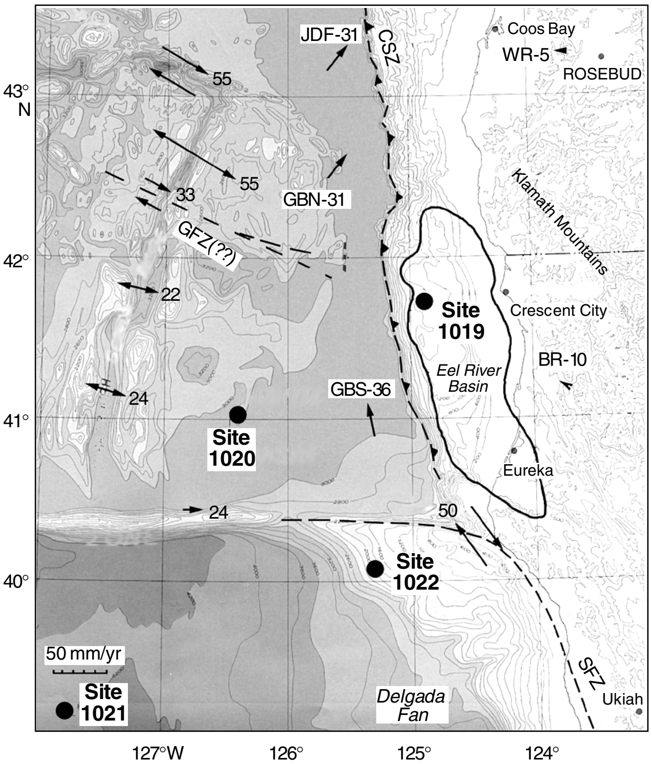

Figure 1. Location of Site 1020. JDF = Juan de Fuca Plate, WR = Willamette Block Rotation, GBN = Gorda Basin North, GBS = Gorda Basin South, GFZ = possible Gorda Fracture Zone, BR = Basin and Range rifting, SFZ = San Andreas Fault Zone, CSZ = Cascadia Subduction Zone (from Shipboard Scientific Party, 1997).

iment diagenesis (Volkman et al., 1980; Brassell et al., 1986; Prahl et al., 1993; Herbert et al., 1998). Marlowe et al. (1990) identified the coccolithophorid class Prymnesiophyceae as the exclusive photosynthetic algae that biosynthesize alkenones. Brassell et al. (1986) pioneered the use of alkenone paleothermometry and defined a link between alkenone unsaturation and overlying water temperature as the index. Subsequent laboratory culture work by Prahl and Wakeham $U^{k'}_{37}$ (1987) and Prahl et al. (1988) on *Emiliania huxleyi* strain 55a (northeast Pacific) calibrated the $U^{k'}_{37}$ index with algal growth temperatures. Since then, other workers have validated this global calibration with respect to core-top sediments and modern SST (Sikes et al., 1997; Rostek et al., 1993; Doose et al., 1997; Sonzogni et al., 1997; Herbert et al., 1998; Müller et al., 1998), and recent studies have characterized paleo-SST and productivity disturbances within the CCS on Holocene–LGM time scales (Prahl et al., 1993, 1995; Doose et al., 1997; Herbert et al., 1995, 1998). Prahl et al. (1995) and Doose et al. (1997) used $U^{k'}_{37}$-derived SSTs from core-top and LGM sediment samples and documented a warming of 3°–4°C since the LGM at 42°N. Unpublished alkenone results from our lab show that Holocene–LGM SST anomalies varied consistently along the entire California margin (23°–41°N; T.D. Herbert et al., unpubl. data), similar to those determined by most faunal studies. One study (Kennett and Venz, 1995), however, estimated an 8°C LGM–Holocene warming in the Santa Barbara Basin using coiling ratios of *Neogloboquadrina pachyderma*.

Detailed SST records derived from the use of alkenones along the California margin were first published by Prahl et al. (1993). They used data from the Multitracers project to relate alkenone-based SST to modern SST or photic zone temperatures and, at a site ~1°N of Site 1020, found that alkenone-based SST most closely represents winter SST or annual average temperatures at 50 m. Herbert et al. (1998) showed that along the continental margin (water depth <2 km), alkenone-derived SSTs from both *Gephyrocapsa oceanica* and *E. huxleyi* most closely relate to mean annual surface temperatures. These studies used numerous core-top samples to conclude that alkenone-derived SSTs exhibit a systematic bias of colder temperatures toward the gyre of up to ~3°C, which may reflect changes in seasonality or depth of production.

We present here an alkenone-proxy record of SST and Haptophyte algal productivity at ODP Site 1020, and we discuss our results with respect to those from other sites along the California margin (Herbert et al., 1995; Prahl et al., 1995; Sabin and Pisias, 1996; Doose et al., 1997; Ortiz et al., 1997). Site 1020 provides the opportunity to assess the scale of SST anomalies and their relationships to Haptophyte productivity and global ice volume well beyond the LGM. Our record extends over eight glacial–interglacial cycles to the Brunhes/Matuyama magnetic reversal boundary (780 ka) and thus represents one of the longest paleoceanographic records available from the California margin.

OCEANOGRAPHIC SETTING

The CCS consists of three distinct currents: (1) the California Current, flowing southward with a dispersed, eddy-ridden character that typifies eastern boundary surface currents (Hickey, 1979); (2) the subsurface California Countercurrent, flowing northward in a more focused manner than the diffuse, turbulent California Current, although little is known of its influence north of San Francisco (Hickey, 1979; Karlin, 1980); and (3) the surface Davidson Current, flowing northward along the coast north of Point Conception (~35°N), but only during fall and winter (Hickey, 1979). Some workers (e.g., Smith, 1992) have suggested that the Davidson Current may represent the surface manifestation of the California Countercurrent, and water property measurements seem to support this idea (Hickey, 1979). The onset of the Davidson Current during winter further suppresses upwelling along the northern California margin; otherwise, its oceanography is poorly understood.

On seasonal time scales, changes in the intensity and orientation of flow within the CCS reflect the influence of basinwide wind patterns (Fig. 2; Huyer, 1977, 1983). The strength of the gradient between the North Pacific high and the continental thermal low pressure system over California drives local surface winds, which blow weakly from the north, south of Mendocino (Huyer, 1983). These southward winds initiate Ekman transport in the surface layer, resulting in elevated sea-surface topography, depressed isopycnals in the gyre, and the upwelling of cool, saline, nutrient-rich waters along the coast (Huyer, 1983).

On interannual time scales, changes in the CCS reflect the influence of ENSO events that originate in the equatorial Pacific (Chelton, 1981). During El Niño conditions, warmer water propagates northward along the western margin of North America (Simpson, 1983; Emery and Hamilton, 1985; Johnson and O'Brien, 1990; Lyle et al., 1992; Van Scoy and Druffel, 1993; Ramp et al., 1997). This warm-water intrusion changes the overall density field of the surface water, reduces upwelling along the coast of California, and results in lower sediment alkenone and marine C_{org} concentrations. In fact, previous very high-resolution $U^{k'}_{37}$-SST reconstructions show evidence of these subdecadal scale (3–5 yr) phenomena (Kennedy and Brassell, 1992; Herbert et al., 1998). On the glacial–interglacial time scales seen at Site 1020, the opposite scenario may exist, coupling warmest $U^{k'}_{37}$-SST with highest concentrations of alkenones in the sediments.

MATERIALS AND METHODS

We obtained a high-resolution suite of samples (~25-cm intervals; ΔT = 2.5 k.y.) from the upper 85 meters composite depth (mcd) of

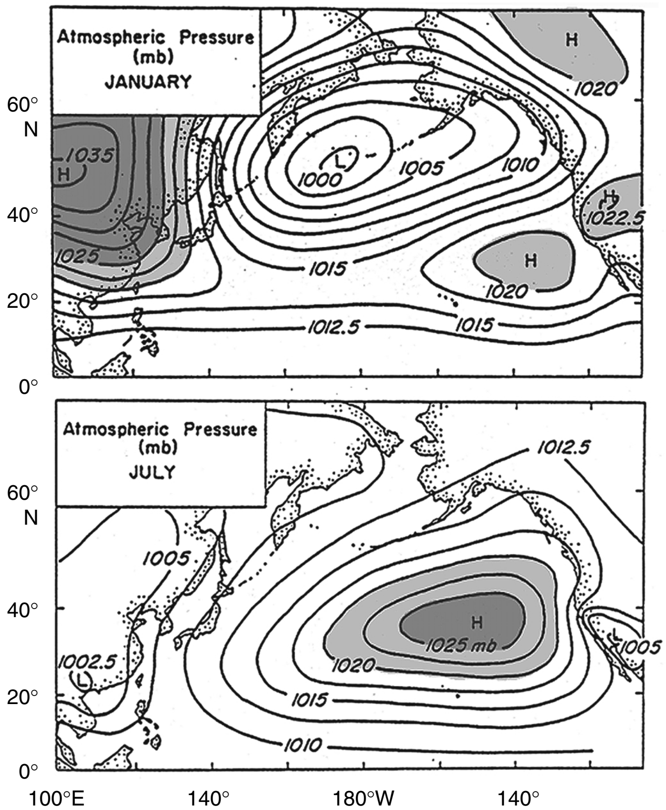

Figure 2. Surface atmospheric pressure for winter and summer (from Huyer, 1983; mb = millibar).

sediment at Site 1020 (41°N, 126°W), with overlap between Holes 1020C and 1020D to ensure a complete record (Fig. 3). All sediment samples were treated and analyzed for alkenones according to the methods described in Herbert et al. (1998). We routinely obtained a precision of better than 0.005 $U^{k'}_{37}$ units (~0.15°C) as determined by replicate analyses of selected sediment samples. Comparison of core-top and LGM $U^{k'}_{37}$-SSTs from Prahl et al. (1995), Doose et al. (1997), Herbert et al. (1998), and this study show excellent agreement between the two labs.

Some workers disagree about whether to include the tetra-unsaturated ketone ($C_{37:4}$) in temperature estimations (Prahl et al., 1988, 1993; Sikes et al., 1997; Brassell, 1993; Conte and Eglinton, 1993; Rosell-Melé et al., 1993). The $U^{k'}_{37}$ calibration neglects the $C_{37:4}$ ketone from SST estimates. At Site 1020, this particular molecule occurs in greatest abundance during glacial phases, but it often coelutes with unknown molecules, making it difficult to reproduce analytically. Consequently, many calibration studies favor the use of $U^{k'}_{37}$ indices along the California margin (Prahl et al. 1988; Doose et al., 1997; Herbert et al., 1998) and in colder regions such as the Southern Ocean (Sikes et al., 1997), and we report only the $U^{k'}_{37}$ index in Table 1.

All of our glacial-age samples contain di-, tri-, and tetra-unsaturated alkenones ($C_{37:2}$, $C_{37:3}$, $C_{37:4}$), whereas interglacial-age samples contain only di- and tri-unsaturated alkenones. This reflects the greater importance of $C_{37:4}$ molecules at cooler SSTs (Brassell et al., 1986; Rosell-Melé et al., 1993). We calculate alkenone concentrations (SC_{37}; nmol/g dry sediment) as the sum of the $C_{37:2}$, $C_{37:3}$, and $C_{37:4}$ molecules, and we assume that SC_{37} represents a proxy for Haptophyte algal productivity (Villanueva et al., 1997; Rosell-Melé et al., 1997). These concentrations reflect the productivity and preservation of one important component of marine phytoplankton, subject to dilution from other sources.

Numerous laboratory culture and core-top experiments (Prahl and Wakeham, 1987; Brassell, 1993; Volkman et al., 1995) have shown that the $U^{k'}_{37}$ index faithfully records modern SST (Fig. 4, inset). We believe that these results validate our choice to present our SST reconstruction using the $U^{k'}_{37}$ index for this region.

AGE MODEL

We assigned preliminary ages to our samples from paleomagnetic identification of the Brunhes/Matuyama Chron (81.21 mcd; Heider et al., Chap. 28, this volume) and assuming a constant sedimentation rate of ~10 cm/k.y. The complete $\delta^{18}O$ record from Site 1020 is not yet available as this is written. Data are available for isotope Stages 1.0–3.3, 5.1–6.4, 7.1–8.4, and 8.5–10.2 (A. Mix, pers. comm., 1998). Our spliced record (Fig. 3) bears a striking resemblance to ice-volume changes as inferred from SPECMAP $\delta^{18}O$ and other Brunhes Chron $\delta^{18}O$ records. We have matched our $U^{k'}_{37}$ SST estimates to the SPECMAP composite (Imbrie et al., 1984), Site 677 (Shackleton et al., 1990), and to the preliminary benthic $\delta^{18}O$ record from Site 1020 (A. Mix, pers. comm., 1998). The most striking feature is the cooccurrence of maximum $U^{k'}_{37}$ SST and interglacial $\delta^{18}O$. This correlation is documented directly at Site 1020 for benthic $\delta^{18}O$ Stages 5.1–5.5 and 7.1–8.4 (A. Mix, pers. comm., 1998). Based on this relationship between warmest $U^{k'}_{37}$ SST and lightest benthic $\delta^{18}O$, we tied our warmest $U^{k'}_{37}$ SSTs from Site 1020 with Site 677 interglacial $\delta^{18}O$ (Shackleton et al., 1990) at Stages 5.5, 7.0, 9.0, 11.1, 15.1, 15.3, 17.0, and 19.0. We linearly interpolated ages using the Site 677 time scale (Shackleton et al., 1990) between oxygen isotope Stages (OIS) 5.5, 7.0, 11.1, 15.1, 15.3, and 17.0 at Site 677 and the Brunhes/Matuyama boundary at Site 1020 (Fig. 5). We remind the reader that Site 677 $\delta^{18}O$ is used only because its length is similar to our alkenone record. Our references to "leads" or "lags" are speculative, but we are confident that we will observe similar phase relationships with the complete Site 1020 $\delta^{18}O$ record when it becomes available.

RESULTS

Our record of alkenone concentration and $U^{k'}_{37}$ SST at Site 1020 shows dominant 100-k.y. glacial–interglacial cyclicity over the last 780 k.y. Global ice volume has a strong 100-k.y. component, and comparisons of our data with benthic $\delta^{18}O$ should enable us to examine phase relationships between alkenone-based SST, alkenone concentration, and $\delta^{18}O$. Over the last four major glacial–interglacial cycles, glacial temperatures have reached remarkably consistent minima (~6°C). These temperatures exist today in the Gulf of Alaska (Levitus, 1994). Deglacial warming has averaged 7°–10°C over this period; however, peak interglacial temperatures show larger variation than full glacial conditions. Alkenone temperature estimates suggest that three of the last four interglacial periods have been 2°–3°C warmer than the Holocene. Earlier in the record, the average $U^{k'}_{37}$ index increases noticeably in a manner consistent with overall warmer marine temperatures in the first half of the Brunhes Chron. Peak interglacial temperatures do not appear any warmer than the interglacials of the latest Pleistocene, and glacial sea-surface cooling was reduced (Fig. 5). Despite the overall similarity between alkenone SST and global ice-volume records, the timing of coldest SSTs along the northern California margin precedes greatest global ice volume by ~8–10 k.y. For example, during the last glacial cycle at Site 1020, minimum SSTs occurred at ~30 ka (OIS 3), ~9 k.y. before the LGM. A similar, though less well-constrained, early warming occurred at Site 1020 in each of the last four glacial–interglacial cycles.

Alkenones derive exclusively from phytoplankton, hence their concentration in marine sediments reflects the supply and preservation of marine organic matter. Studies have shown that organic carbon supply plays a more important role than preservation in determin-

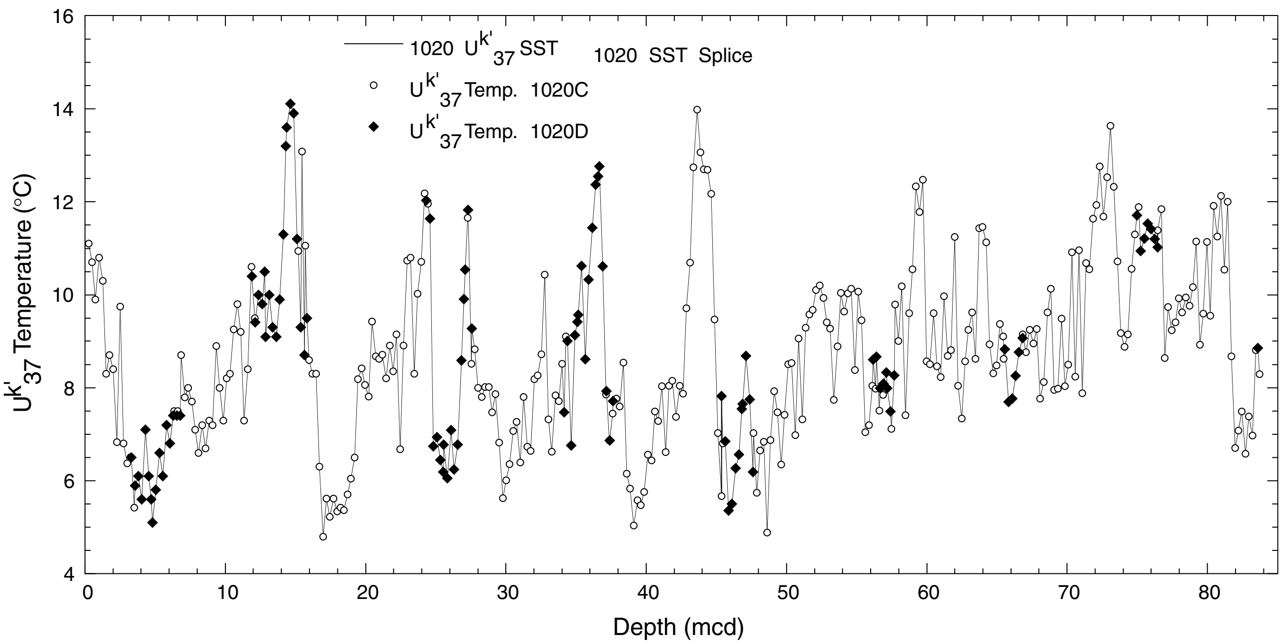

Figure 3. Alkenone splice time series from Holes 1020C and 1020D. SST = sea-surface temperatures.

Table 1. Alkenone data from Site 1020.

Hole	Core, section	Interval (cm)	Depth (mcd)	$U^{k'}_{37}$ index	$U^{k'}_{37}$ temp. (°C)	ΣC_{37} (nmol/g)
1020C	1H-1	025-026	0.25	0.418	11.1	2.70
	1H-1	050-051	0.50	0.403	10.7	1.69
	1H-1	075-076	0.75	0.375	9.9	1.77
	1H-1	100-101	1.00	0.407	10.8	3.11
	1H-1	125-126	1.25	0.390	10.3	2.26
	1H-2	000-001	1.50	0.320	8.3	2.32
	1H-2	025-026	1.75	0.335	8.7	1.10
	1H-2	050-051	2.00	0.326	8.4	0.79
	1H-2	075-076	2.25	0.272	6.8	1.58
	1H-2	100-101	2.50	0.370	9.8	0.20

Note: temp. = temperature.

This is a sample of the table that appears on the volume CD-ROM.

ing the total fraction of marine C_{org} in sediments (Karlin et al., 1992; Reimers et al., 1992; Dean et al., 1994). Total organic carbon measurements are useful in assessing marine productivity rates (Müller and Suess, 1979; Eppley and Peterson, 1979; Rabouille and Gaillard, 1991); however, terrigenous C_{org} may comprise a significant portion of the total C_{org} in continental margin sediments. To develop a history of paleoproductivity along the northern California margin, we must estimate the marine fraction of C_{org} over time. We do not expect SC_{37} and marine C_{org} to correlate perfectly because other marine plankton groups may contribute significant fractions of the total C_{org}. A comparison of SC_{37} and $U^{k'}_{37}$ SST shows that higher alkenone concentrations occur during interglacials than during glacial periods (Fig. 6). Although the time series of SC_{37} and $CaCO_3$ (Lyle et al., Chap. 11, this volume) are not exactly in phase, comparison of the two records does show some significant similarities (i.e., shared peaks at ~68, ~260, ~360, and ~500 ka). We explore later the relationship between lower inferred coccolithophorid productivity and cold glacial SST estimated at Site 1020. On longer time scales, a general shift to higher SC_{37} values occurs before OIS 13 (~500 ka using our preliminary time scale).

DISCUSSION

We can assess the validity of our results from Site 1020 in several ways. The $U^{k'}_{37}$-SST estimates from our Holocene samples at Site 1020 most closely resemble modern winter SST in the area (Levitus, 1994; Fig. 4). This means that any cooling in our record cannot result from a shift toward a colder season of productivity. Temperatures warmer than Holocene could reflect a bias associated with changes in the seasonal patterns of production toward spring or summer months; however, the Holocene marine isotope Stage (MIS) 5.5 temperature increase at Site 1020 is identical to that at Site 893, which shows no seasonal bias occurring today (Herbert et al., 1995).

The magnitude of glacial–interglacial SST variability holds remarkably constant over the last 450 k.y. with glacial temperatures around 5°C cooler and interglacial SSTs 2°–3°C warmer than today. The LGM–Holocene warming of ~4°C that we infer from Site 1020 also agrees with data from other locations along the California margin. To the south, $U^{k'}_{37}$-SST records at Site 893 (Santa Barbara Basin) and Core EW9504-03PC (32°04′, 117°35′) show ~2°–3°C warming from LGM–Holocene (Fig. 7; Herbert et al., 1995). In all three cases, MIS 5.5 is warmer than modern. To the north, $U^{k'}_{37}$-SST records at Multitracers Site Midway (W8709-8PC and TC) indicate roughly a 5°C warming since the LGM, but unfortunately, this record does not extend to MIS 5.5.

The consistency in glacial–interglacial warming strengthens our confidence in the data and strongly suggests a margin-wide response as climate changed from full glacial to interglacial conditions. Other marine isotopic and faunal studies (Sabin and Pisias, 1996; Ortiz et al., 1997) confirm the alkenone SST warming we see along the California margin, but these records extend only to the LGM.

At Site 1020, profiles of C_{org} and total alkenone concentrations (Lyle et al., Chap. 11, this volume) are greatest around warmest alkenone SSTs from the LGM–Holocene. This inferred increase in sedimentary C_{org} and alkenone concentrations is also seen farther south in alkenone data from Site 893 (Herbert et al., 1995) and in Core EW9504-03PC (T.D. Herbert et al., unpubl. data). To the north, Lyle

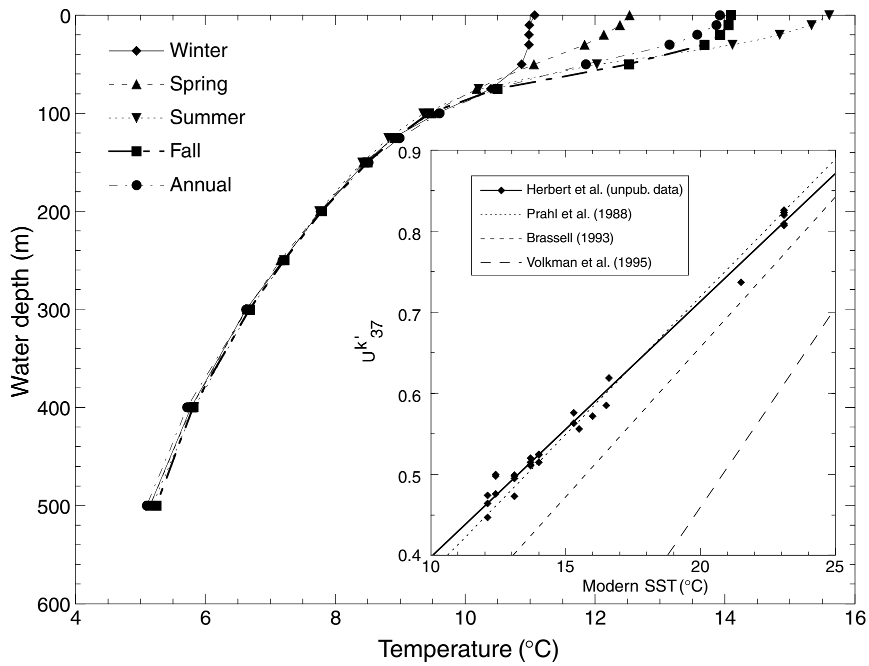

Figure 4. Modern water temperatures at Site 1020 to 500 m water depth. Our youngest $U^{k'}_{37}$ estimate (11.1°C) corresponds to modern winter sea-surface temperatures (SST) or mean annual average at 70 m. Inset is core-top $U^{k'}_{37}$ calibrations vs. modern sea-surface temperature. The robust fit validates our use of the $U^{k'}_{37}$ method to reconstruct SST.

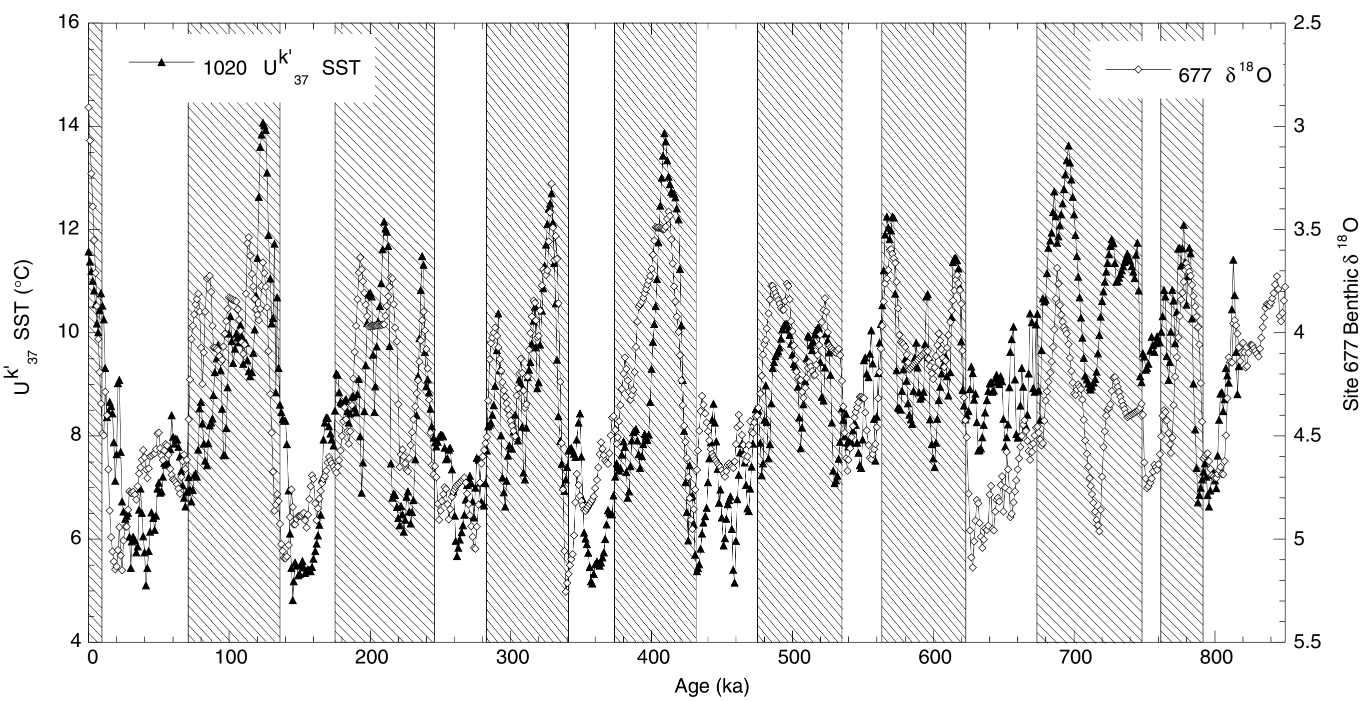

Figure 5. Site 1020 $U^{k'}_{37}$ SST and Site 677 $\delta^{18}O$. Age model from tuning Site 1020 to Site 677 $\delta^{18}O$. Interglacial periods are shaded. SST = sea-surface temperatures.

et al. (1992) saw increases in C_{org} mass accumulation rates since the LGM in the Multitracers Transect. Ortiz et al. (1997) inferred increases in productivity since LGM at 42°N from isotopic gradients in *Gephyrocapsa bulloides* and from planktonic foraminiferal shell accumulation rates. Based on our data from Site 1020 and the data from these earlier studies, we infer that productivity may have been reduced during the LGM and has slowly increased in strength as modern conditions evolved. Terrestrial proxies such as coastal redwood pollen also suggest that upwelling ceased or diminished along the California margin (Heusser, Chap. 20, this volume). Sancetta et al. (1992) analyzed Core W8709-3 from 42°N and found less redwood pollen during the LGM, matching more recent data by Heusser et al. (Chap. 17, this volume). They concluded that weakened summer upwelling was responsible for the decreases in pollen. At Site 1020, correlations between redwood pollen and alkenone SST also suggest that upwelling was strongest during interglacial periods and weaker or nonexistent during glacial periods (Heusser et al., Chap. 17, this volume).

In addition to observed LGM–Holocene SST warming and Haptophyte productivity increases, alkenone SST records along the California margin also show similar relationships to ice volume. The coldest alkenone SSTs at Sites 1020 and 893 and Core EW9504-03PC all lead $\delta^{18}O$ maximum ice volume by at least 5 k.y. (Fig. 7; Herbert et al., 1995) in the south, and we speculate by a similar amount at Site 1020 in the north. The geographic consistency of this relationship suggests that there is an early response of SST warming with respect to ice volume along the California margin. The length of our record at Site 1020, coupled with the Site 893 record (Herbert et al., 1995), allows us for the first time to infer the behavior of sea-surface temperatures within the CCS beyond the last glacial period. We see that this early deglacial warming occurs consistently over ~350 k.y.; however, we are less confident in the preliminary age model much beyond this point.

A margin-wide SST response along the California margin would require a large-scale forcing during a glacial–interglacial transition. Two proposed mechanisms for cooler SSTs involve contributions from atmospheric effects resulting from the presence of glacial ice sheets and/or changes in thermohaline transport within the CCS.

An expansion of the Alaskan Gyre southward, perhaps because of changes in either oceanic or atmospheric circulation patterns, would aid in cooling the sea surface of the northeast Pacific Ocean. This encroachment of cool, subarctic water in the glacial northeast Pacific is similar to the scenario proposed by CLIMAP Project Members (1981) in the LGM North Atlantic, which shows the deflection of the Gulf Stream by the advancing polar front in the glacial North Atlantic. The expansion may have deflected the North Pacific Current/Kuroshio Current Extension and the west wind drift to the south, allowing cooler temperatures to exist for a longer duration in the northern part of the CCS.

A map of the southernmost extent of ice-rafted debris (IRD) in the northeast Pacific (Fig. 8) provides evidence independent of alkenone estimates that a cooler northeast Pacific existed during glacial times. ODP Site 887 (Gulf of Alaska) shows a large range in IRD abundance (Krissek, 1995) preserved there, and references to IRD as far south as off the coast of Oregon are made in Griggs and Kulm (1969). These deposits suggest that major ice sources must have been located proximal to the Gulf of Alaska and offshore of the northwest coast of North America during glacial times. Thus, the presence of IRD in the northeast Pacific supports the notion that the icebergs must have originated there. The petrology of the Site 887 IRD suggests that the provenance was the Alaskan coastal region and the Pacific Northwest of North America (Krissek, 1995). If SSTs in present areas of sea ice are analogs of the past, water temperatures proximal to sea ice would have been on the order of 2°–4°C (CLIMAP, 1981) for the LGM northern northeast Pacific. Therefore, the glacial temperatures as cold as 4°–6°C at Site 1020 are plausible.

The southward expansion of the northeast Pacific IRD belt is not necessarily the ultimate mechanism for glacial cooling of the sea surface. What could cause this belt to expand? For the IRD belt to propagate southward, the sea surface must be cool enough to allow the southerly migration of ice. COHMAP Members (1988) have modeled the atmospheric surface winds for the Holocene and LGM, and their results suggest an increase in the influence of the Aleutian Low, typically seen in modern Northern Hemisphere winter (Fig. 2; Huyer, 1983). We believe that the persistence of cyclonic wind fields over the northeast Pacific Ocean may have played a part in increasing the size

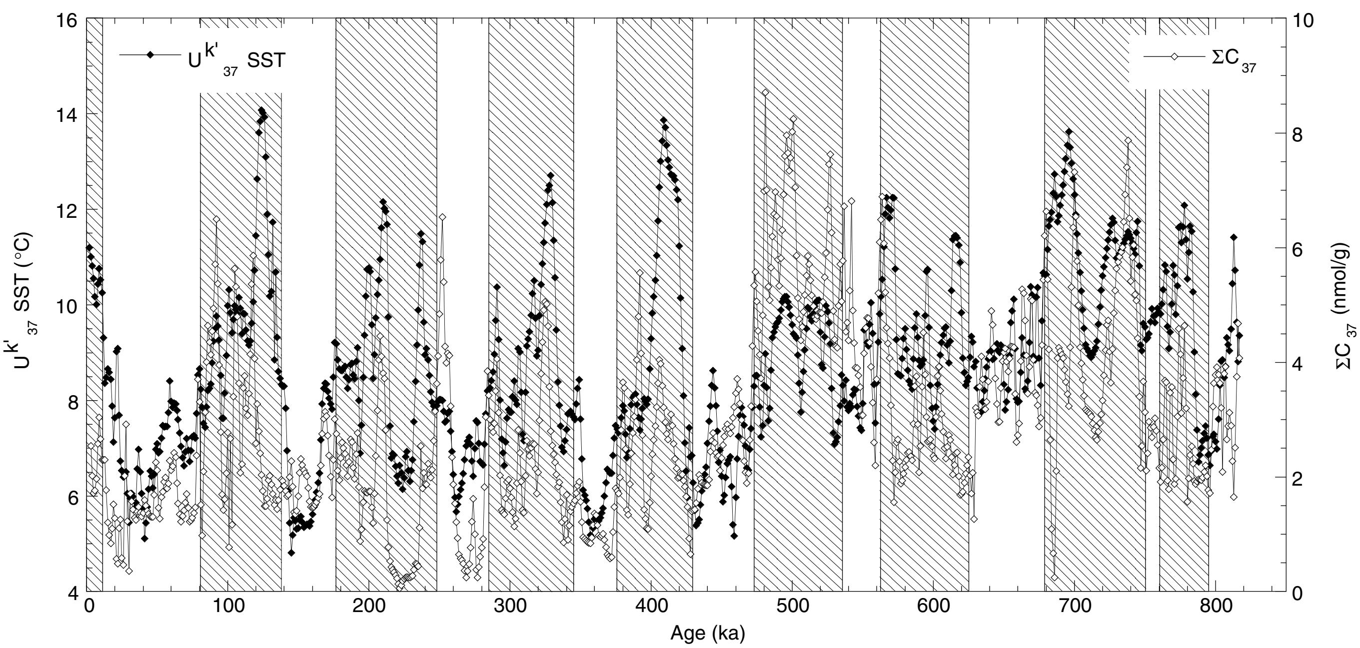

Figure 6. Site 1020 $U^{k'}_{37}$ SST and alkenones concentration on time scale developed from Site 677 $\delta^{18}O$. Interglacial stages are shaded. SST = sea-surface temperatures.

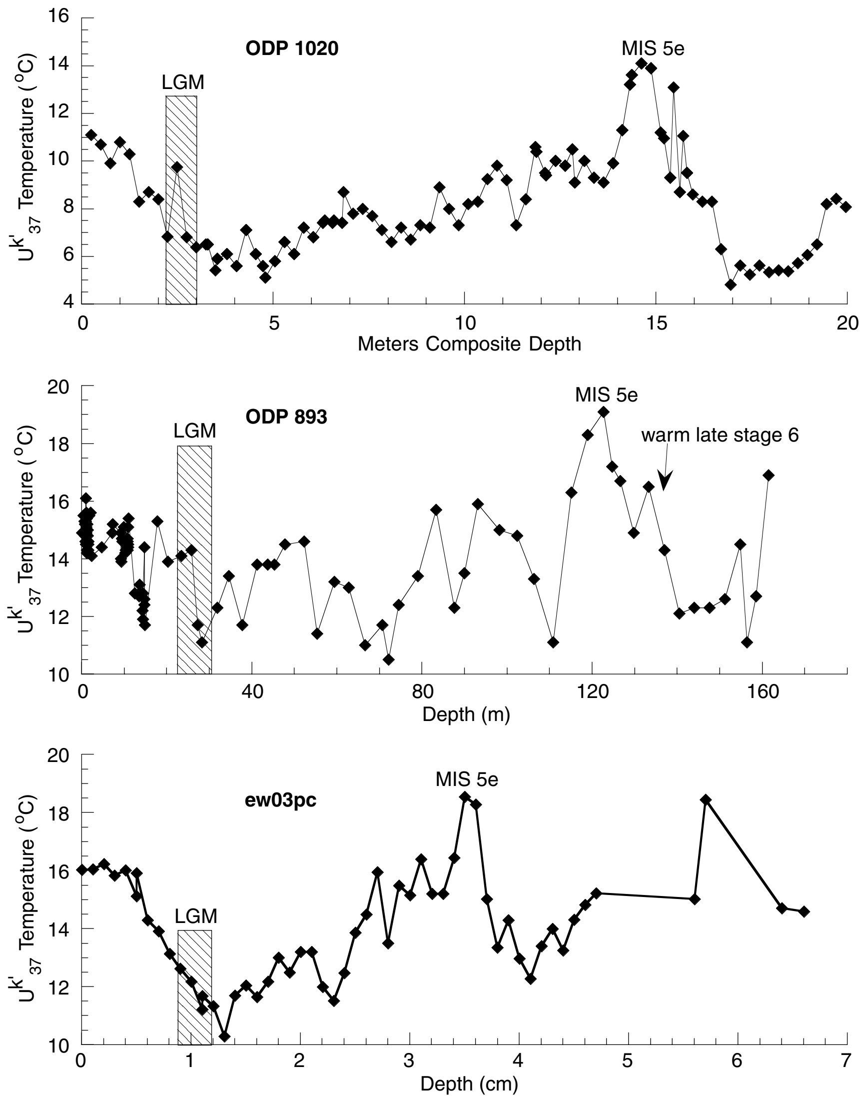

Figure 7. Milankovitch-scale resolution records from Holes 1020 (north) and 893 (central), and Core EW9504-03PC (southern) along the California margin. Benthic $\delta^{18}O$ confirms positions of last glacial maximum (LGM) and marine isotope Substage (MIS) 5e in all locations (Site 1020: A. Mix, pers. comm., 1998; Site 893: Kennett et al., 1995; Core EW9504-03PC: L. Stott, pers. comm., 1998). Shaded region defines the LGM time interval (21 ± 2 ka).

of the Alaskan Gyre, causing its sphere of influence to be felt farther south than today. The idea of the southerly migration of the Alaskan Gyre is not new. Moore (1973), who documented subarctic radiolarian fauna along the northern California/southern Oregon border, was first to propose that Alaskan fauna existed this far south during the LGM. Lyle et al. (1992) acknowledged the possibility of the Alaskan Gyre planktonic community thriving off the coast of Oregon based upon productivity and organic carbon fluxes along the Multitracers Transect at 42°N. However, Lyle et al. (1992) suggested reduced coastal upwelling or subsurface replacement of nutrient-rich water as a better explanation of their data. Ortiz et al. (1997), using transfer functions from a 10-core transect at 42°N, saw that the strongest modern analogs of glacial fauna currently live in the Alaskan Gyre.

The northward winds modeled by COHMAP Members (1988) for the LGM along the California margin would have reduced upwelling at Site 1020. We see this reduction evidenced by lower C_{org}, terrestrial pollen, and SC_{37} concentrations. One factor that may have contributed to the reduction of upwelling is an increase in northward, coastal flow of the geostrophic Davidson Current (Hickey, 1979), which would be possible under the atmospheric scenario proposed by COHMAP Members (1988).

We must also consider the possibility that a disturbance in the heat budget of the tropics and higher latitudes existed during the LGM, as suggested by Sr/Ca measurements of corals (Beck et al., 1992). If the tropical LGM anomaly was as large as this method predicts, this disturbance would have serious consequences regarding thermohaline reorganization along the California margin.

The modern relationship of colder SST and enhanced upwelling/organic preservation (La Niña) and anomalously warm SST with reductions in upwelling (ENSO) along the California margin does not persist on an orbital time scale. The increases in the records of sedimentary alkenone concentration, C_{org}, and terrestrial pollen assemblages all center around warmer SSTs at Site 1020. From this, we have inferred maximum productivity or preservation of sediment alkenone concentrations during warmer periods of SST, although periods that are more productive have existed during the past (for example, OIS 13).

CONCLUSIONS

We present here the 780-k.y. $U^{k'}_{37}$-SST and alkenone productivity record at Site 1020. We have made the following conclusions:

1. Glacial–interglacial SST amplitudes have varied consistently over the last 450 k.y.; however, the total amplitude dampens

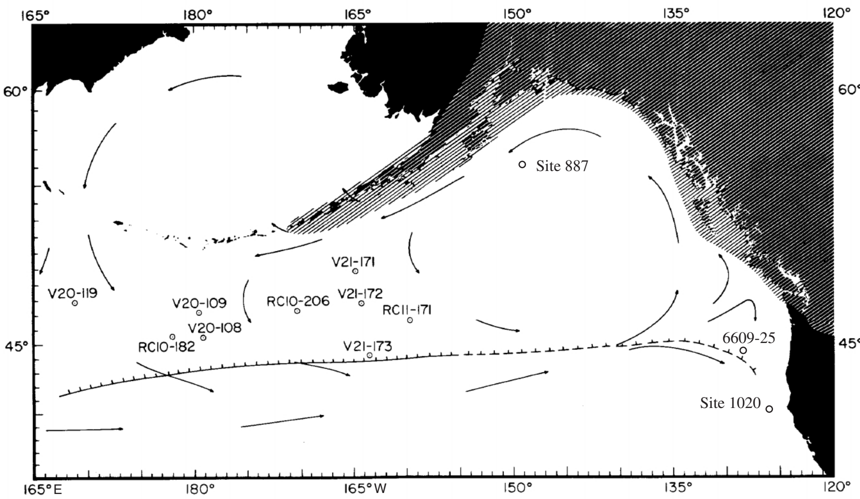

Figure 8. Limits of IRD in the northeast Pacific. Figure modified from Kent et al. (1971) with data from Hole 887 (Krissek, 1995) and Site 6609-25 (Griggs and Kulm, 1969). Hatched lines on continent are limit of continental ice. Hatched line in the ocean is limit of glacial marine sediments, as mapped by Conolly and Ewing (1970), Kent et al. (1971), and Griggs and Kulm (1969). Modern surface circulation depicted by arrows. Site 1020 is shown to orient the reader.

during the early Brunhes Chron. Also, interglacial SSTs are generally warmer than Holocene values by ~3°C.

2. Our Holocene–LGM SST decrease of 5°C is within the error of previous multiproxy studies such as Prahl et al. (1995), Sabin and Pisias (1996), and Ortiz et al. (1997).
3. The sea-surface glacial cooling of 5°C at Site 1020 may be the result of the complex interaction of this current system with sea ice, glacial atmospheric effects, and a southward expansion of the Alaskan Gyre in the glacial northeast Pacific. Our Holocene $U^{k'}_{37}$-based SSTs most closely approximate modern winter SST (or subsurface production); therefore, the only possible bias (relative to today) would involve a shift to a warmer season of production.
4. We infer a tight correlation between warmest alkenone SST and minimum ice volume over the last 800 k.y. This cannot be tested adequately until a suite of $\delta^{18}O$ data from Site 1020 at the same resolution become available. We observe similar relationships between alkenone's SST and $\delta^{18}O$ data in cores to the south (Herbert et al., 1995; T.D. Herbert et al., unpubl. data).
5. The paleoceanographic record at Site 1020 shows evidence for enhanced Haptophyte productivity during periods of warm SST and diminished productivity during cold SST. This inferred productivity pattern is consistent with sedimentary C_{org} content and with climatic information from redwood pollen (Heusser, Chap. 20, this volume).

ACKNOWLEDGMENTS

This research was supported in part by a JOI/USSAC grant. We thank the Ocean Drilling Program and the Leg 167 Scientific Party. Reviews by Drs. Mitch Lyle, Ralph Schneider, and an anonymous reviewer greatly aided the final draft of this paper.

REFERENCES

Beck, J.W., Edwards, R.L., Ito, E., Taylor, F.W., Recy, J., Rougerie, F., Joannot, P., and Henin, C., 1992. Sea-surface temperature from coral skeleton strontium/calcium ratio. *Science,* 257:644–647.

Brassell, S.C., 1993. Applications of biomarkers for delineating marine paleoclimatic fluctuations during the Pleistocene. *In* Engel, M.H., and Macko, S.A. (Eds.), *Organic Geochemistry: Principles and Applications:* New York (Plenum), 699–738.

Brassell, S.C., Eglinton, G., Marlowe, I.T., Pflaumann, U., and Sarnthein, M., 1986. Molecular stratigraphy: a new tool for climatic assessment. *Nature,* 320:129–133.

Chelton, D.B., 1981. Interannual variability of the California Current: physical factors. *Calif. Coop. Fisher. Investig.,* 22:34–48.

Chelton, D.B., 1982. Large-scale response of the California Current to forcing by the wind stress curl. *Calif. Coop. Fisher. Invest.,* 23:130–148.

CLIMAP Project Members, 1981. Seasonal reconstructions of the Earth's surface at the last glacial maximum. *Geol. Soc. Am., Map and Chart Ser.,* MC36.

COHMAP Members, 1988. Climatic changes of the last 18,000 years: observations and model simulations. *Science,* 241:1043–1052.

Conolly, J.R., and Ewing, M., 1970. Ice-rafted detritus in northwest Pacific deep-sea sediments. *In* Hays, J.D. (Ed.), *Geological Investigations of the North Pacific.* Mem.—Geol. Soc. Am., 126:219–231.

Conte, M.H., and Eglinton, G., 1993. Alkenones and alkenoate distributions within the euphotic zone of the eastern North Atlantic: correlation with production temperature. *Deep-Sea Res.,* 40:1935–1961.

Dean, W.E., Gardner, J.V., and Anderson, R.Y., 1994. Geochemical evidence for enhanced preservation of organic matter in the oxygen minimum zone of the continental margin of northern California during the late Pleistocene. *Paleoceanography,* 9:47–61.

Dettinger, M.D., Ghil, M., and Keppenne, C.L., 1995. Interannual and interdecadal variability in United States air temperatures, 1910–87. *Climate Change,* 31:35–66.

Doose, H., Prahl, F.G., and Lyle, M.W., 1997. Biomarker temperature estimates for modern and last glacial surface waters of the California Current system between 33° and 42°N. *Paleoceanography,* 12:615–622.

Emery, W.J., and Hamilton, K., 1985. Atmospheric forcing of interannual variability in the northeast Pacific Ocean: connections with El Niño. *J. Geophys. Res.,* 90:857–868.

Enfield, D.B., 1989. El Niño—past and present. *Rev. Geophys.,* 27:159–187.

Eppley, R.W., and Peterson, B.J., 1979. Particulate organic matter flux and planktonic new production in the deep ocean. *Nature,* 282:677–680.

Griggs, G.B., and Kulm, L.D., 1969. Glacial marine sediments from the northeast Pacific. *J. Sediment. Petrol.,* 39:1142–1148.

Hayward, T.L., Cummings, S.L., Cayan, D.R., Chavez, F.P., R.J. Lynn, R.J., Mantyla, A.W., Niiler, P.P., Schwing, F.B., Veit, R.R., and Venrick, E.L., 1996. The state of the California current in 1995–96: continuing declines in macrozooplankton biomass during a period of nearly normal circulation. *CalCOFI Rep.,* 37.

Herbert, T.D., Schuffert, J.D., Thomas, D., Lange, K., Weinheimer, A., and Herguera, J.-C., 1998. Depth and seasonality of alkenone production along the California margin inferred from a core-top transect. *Paleoceanography,*13:263–271.

Herbert, T.D., Yasuda, M., and Burnett, C., 1995. Glacial-interglacial sea-surface temperature record inferred from alkenone unsaturation indices, Site 893, Santa Barbara Basin. *In* Kennett, J.P., Baldauf, J.G., and Lyle, M. (Eds.), *Proc. ODP, Sci. Results,* 146 (Pt. 2): College Station, TX (Ocean Drilling Program), 257–264.

Hickey, B.M., 1979. The California Current System: hypotheses and facts. *Prog. Oceanogr.,* 8:191–279.

Huyer, A., 1977. Seasonal variation in temperature, salinity, and density over the continental shelf off Oregon. *Limnol. Oceanogr.,* 22:442–453.

Huyer, A., 1983. Coastal upwelling in the California Current system. *Prog. Oceanogr.,* 12:259–284.

Imbrie, J., Hays, J.D., Martinson, D.G., McIntyre, A., Mix, A.C., Morley, J.J., Pisias, N.G., Prell, W.L., and Shackleton, N.J., 1984. The orbital theory of Pleistocene climate: support from a revised chronology of the marine $\delta^{18}O$ record. *In* Berger, A., Imbrie, J., Hays, J., Kukla, G., and Saltzman, B. (Eds.), *Milankovitch and Climate* (Pt. 1), NATO ASI Ser. C, Math Phys. Sci., 126:269–305.

Johnson, M.A., and O'Brien, J.J., 1990. The northeast Pacific Ocean response to the 1982-1983 El Niño. *J. Geophys. Res.,* 95:7155–7166.

Karlin, R., 1980. Sediment sources and clay mineral distributions off the Oregon coast. *J. Sediment. Petrol.,* 50:543–560.

Karlin, R., Lyle, M., and Zahn, R., 1992. Carbonate variations in the Northeast Pacific during the late Quaternary. *Paleoceanography,* 7:43–61.

Kennedy, J.A., and Brassell, S.C., 1992. Molecular records of twentieth century El-Niño events in laminated sediments from the Santa Barbara basin. *Nature,* 357:62–64.

Kennett, J.P., and Venz, K., 1995. Late Quaternary climatically related planktonic foraminiferal assemblage changes: Hole 893A, Santa Barbara Basin, California. *In* Kennett, J.P., Baldauf, J.G., and Lyle, M. (Eds.), *Proc. ODP, Sci. Results,* 146 (Pt. 2): College Station, TX (Ocean Drilling Program), 281–293.

Kent, D.V., Opdyke, N.D., and Ewing, M., 1971. Climate change in the North Pacific using ice-rafted detritus as a climatic indicator. *Geol. Soc. Am. Bull.,* 82:2741–2754.

Krissek, L.A., 1995. Late Cenozoic ice-rafting records from Leg 145 sites in the North Pacific: late Miocene onset, late Pliocene intensification, and Pliocene–Pleistocene events. *In* Rea, D.K., Basov, I.A., Scholl, D.W., and Allan, J.F. (Eds.), *Proc. ODP, Sci. Results,* 145: College Station, TX (Ocean Drilling Program), 179–194.

Levitus, S., 1994. Climatological atlas of the world ocean. *NOAA Prof. Pap.,* 13.

Lyle, M., Koizumi, I., Richter, C., et al., 1997. *Proc. ODP, Init. Repts.,* 167: College Station, TX (Ocean Drilling Program).

Lyle, M., Zahn, R., Prahl, F., Dymond, J., Collier, R., Pisias, N., and Suess, E., 1992. Paleoproductivity and carbon burial across the California Current: the Multitracers Transect, 42°N. *Paleoceanography,* 7:251–272.

Marlowe, I.T., Brassell, S.C., Eglinton, G., and Green, J.C., 1990. Long-chain alkenones and alkyl alkenoates and the fossil coccolith record of marine sediments. *Chem. Geol.,* 88:349–375.

Moore, T.C., Jr., 1973. Late Pleistocene-Holocene oceanographic changes in the northeastern Pacific. *Quat. Res.,* 3:99–109.

Müller, P.J., Kirst, G., Ruhland, G., von Storch, I., and Rossell-Mele, A., 1998. Calibration of the alkenone paleotemperature index $U^{k'}_{37}$ based on core-tops from the eastern South Atlantic and the global ocean (60°N-60°S). *Geochim. Cosmochim. Acta,* 62:1757–1772.

Müller, P.J., and Suess, E., 1979. Productivity, sedimentation rate, and sedimentary organic matter in the oceans, I. Organic carbon preservation. *Deep-Sea Res. Part A,* 26:1347–1362.

Norton, J.G., and McLain, D.R., 1994. Diagnostic patterns of seasonal and interannual temperature variation off the west coast of the United States: local and remote large-scale atmospheric forcing. *J. Geophys. Res.,* 99:16,019–16,030.

Ortiz, J., Mix, A., Hostetler, S., and Kashgarian, M., 1997. The California Current of the last glacial maximum: reconstruction at 42 degrees N based on planktonic foraminifera. *Paleoceanography,* 12:191–205.

Prahl, F.G., Collier, R.B., Dymond, J., Lyle, M., and Sparrow, M.A., 1993. A biomarker perspective on prymnesiophyte productivity in the northeast Pacific Ocean. *Deep-Sea Res. Part A*, 40:2061–2076.

Prahl, F.G., Muehlhausen, L.A., and Zahnle, D.L., 1988. Further evaluation of long-chain alkenones as indicators of paleoceanographic conditions. *Geochim. Cosmochim. Acta,* 52:2303–2310.

Prahl, F.G., Pisias, N., Sparrow, M.A., and Sabin, A., 1995. Assessment of sea-surface temperature at 42° N in the California Current over the last 30,000 years. *Paleoceanography,* 10:763–773.

Prahl, F.G., and Wakeham, S.G., 1987. Calibration of unsaturation patterns in long-chain ketone compositions for paleotemperature assessment. *Nature,* 330:367–369.

Rabouille, C., and Gaillard, J.F., 1991. A coupled model representing the deep-sea organic Carbon mineralization and oxygen consumption in surficial sediments. *J. Geophys. Res.,* 96:2761–2776.

Ramp, S.R., McClean, J.L., Collins, C.A., Semtner, A.J., and Hays, K.A.S., 1997. Observations and modeling of the 1991–1992 El Niño signal off central California. *J. Geophys. Res.,* 102:5553–5582.

Reimers, C.L, Jahnke, R.A., and McCorkle, D.C., 1992. Carbon fluxes and burial rates over the continental slope and rise off central California with implications for the global carbon cycle. *Global. Biogeochem. Cycles,* 6:199–224.

Rosell-Melé, A., Carter, J., and Eglinton, G., 1993. Distribution of long-chain alkenones and alkyl alkenoates in marine surface sediments from the North East Atlantic. *Org. Geochem.*, 22:501–509.

Rosell-Melé, A., Maslin, M.A., Maxwell, J.R., and Schaeffer, P., 1997. Biomarker evidence for "Heinrich" events. *Geochim. Cosmochim. Acta,* 61:1671–1678.

Rostek, F., Ruhland, G., Bassinot, F.C., Muller, P.J., Labeyrie, L.D., Lancelot, Y., and Bard, E., 1993. Reconstructing sea surface temperature using $\delta^{18}O$ and alkenone records. *Nature,* 364:319–321.

Sabin, A.L., and Pisias, N.G., 1996. Paleoceanography of the northeast Pacific Ocean for the last 20,000 years and its relationship to climate change in northwestern North America. *Quat. Res.,* 46:48–61.

Sancetta, C., Lyle, M., Heusser, L., Zahn, R., and Bradbury, J.P., 1992. Late-glacial to Holocene changes in winds, upwelling, and seasonal production of the Northern California current system. *Quat. Res.,* 38:359–370.

Shackleton, N.J., Berger, A., and Peltier, W.A., 1990. An alternative astronomical calibration of the lower Pleistocene timescale based on ODP Site 677. *Trans. R. Soc. Edinburgh: Earth Sci.,* 81:251–261.

Sikes, E.L., Volkman, J.K., Robertson, L.G., and Pichon, J.-J., 1997. Alkenones and alkenes in surface waters and sediments of the Southern Ocean: Implications for paleotemperature estimation in polar regions. *Geochim. Cosmochim. Acta,* 61:1495–1505.

Simpson, J.J., 1983. Large-scale thermal anomalies in the California Current during the 1982–1983 El Niño. *Geophys. Res. Lett.,* 10:937–940.

Smith, R.L., 1992. Coastal upwelling in the modern ocean. *In* Summerhayes, C.P., Prell, W.L., and Emeis, K.C. (Eds.), *Upwelling Systems: Evolution Since the Early Miocene.* Geol. Soc. Spec. Publ. London, 64:9–28.

Shipboard Scientific Party, 1997. Leg 167 introduction. *In* Lyle, M., Koizumi, I., Richter, C., et al., *Proc. ODP, Init. Repts.,*167: College Station, TX (Ocean Drilling Program), 5–13.

Sonzogni, C., Bard, E., Rostek, F., Dollfus, D., Rosell-Mele, A., and Eglinton, G., 1997. Temperature and salinity effects on alkenone ratios measured in surface sediments from the Indian Ocean. *Quat. Res.,* 47:344–355.

Van Scoy, K.A., and Druffel, E.R.M., 1993. Ventilation and transport of thermohaline and intermediate waters in the Northeast Pacific during recent El Niños. *J. Geophys. Res.,* 98:18,083–18,088.

Villanueva, J., Grimault, J.O., Cortijo, E., Vidal, L., and Labeyrie, L., 1997. A biomarker approach to the organic matter deposited in the North Atlantic during the last climate cycle. *Geochim. Cosmochim. Acta,* 61:4633–4646.

Volkman, J.K., Barrett, S.M., Blackburn, S.I., and Sikes, E.L., 1995. Alkenones in Gephyrocapsa oceanica: implications for studies of paleoclimate. *Geochim. Cosmochim. Acta,* 59:513–520.

Volkman, J.K., Eglinton, G., Corner, E.D.S., and Sargent, J.R., 1980. Novel unsaturated straight-chain C_{37}–C_{39} methyl and ethyl ketones in marine sediments and a coccolithophore *Emiliania huxleyi. In* Douglas, A.G., and Maxwell, J.R. (Eds.), *Advances in Organic Geochemistry 1979:* Oxford (Pergamon Press), 219–228.

Date of initial receipt: 27 October 1998
Date of acceptance: 25 August 1999
Ms 167SR-213